A highly scalable path-following controller for N-trailers with off-axle hitching[☆]

Maciej Marcin Michałek

Chair of Control and Systems Engineering, Poznań University of Technology (PUT), Piotrowo 3A, 60-965 Poznań, Poland

This is the accepted author manuscript of the paper published in Control Engineering Practice 29:61-73, 2014, DOI: 10.1016/j.conengprac.2014.04.001

Abstract

The paper presents a highly scalable nonlinear cascaded-like path-following feedback controller for N-trailer robotic vehicles equipped with arbitrary number of off-axle hitched trailers. In contrast to the other path-following control laws proposed in the literature for N-trailer robots, the presented control approach does not require determination of the shortest distance to a reference path. By introducing the so-called *segment-platooning* reference paths, and under the *sign-homogeneity* assumption for hitching offsets, the asymptotic following is guaranteed for both constant- and varying-curvature reference paths using either backward or forward vehicle motion strategy with a guidance point fixed on the last trailer. The paper contains experimental results obtained with a 3-trailer laboratory-scale vehicle.

Keywords: cascaded-like control, path following, N-trailer, off-axle hitching

1. Introduction

The N-trailer vehicles (N-trailers), comprising of a tractor and passively interconnected trailers, are especially interesting systems of exceptional practical meaning [9, 21]. Three kinds of N-trailers with non-steerable axles are distinguished in the literature: Standard N-Trailers (SNT) equipped solely with on-axle joints (mounted on the preceding wheel-axles) [20, 25], non-Standard N-Trailers (nSNT) with all the joints of off-axle type (mounted off the preceding wheel-axles) [14, 32], and General N-Trailers (GNT) where the mixed on-axle and off-axle hitches are present in a vehicle chain [4, 29]. The path-following (PF) control problem for tractor-trailer vehicles has been addressed by numerous researchers within the last two decades. First, because the N-trailers are especially difficult to control as a consequence of their structural properties (see [4, 20, 35]). Second, the PF problem has an important practical meaning in the tasks where the motion geometry is a key factor, while time-execution of the task is secondary [1, 2].

Numerous works on the PF problem have been especially devoted to the robots with strictly limited number of trailers, see e.g. [7, 8, 13, 16, 18, 19, 21, 23, 27, 30, 41, 43, 46]. Feedback-control solutions to the PF problem for truly N-trailers (i.e. admitting arbitrary number of vehicle segments) have been proposed merely in a few works, namely in [48] for SNT robots, in [5, 6, 10] for GNT vehicles, in [9] for nSNT structures, and in [42] for the special kind of N-trailers with steerable axles[1]. Control laws provided in the mentioned works result from application of different mathematical concepts, like the chained-form transformation [48], or various types of linearization [5, 6, 9, 10]. Despite their theoretical soundness and unquestionable elegance, they often provide relatively complex, only locally valid, or hardly scalable control laws, sometimes without clear physical interpretation of particular control components. Mentioned properties may cause serious problems with tuning and implementation of the controllers leading to unacceptable control performance in practical applications. Thus it seems, there is still a need for further investigations in this area to provide new solutions with improved functionality in the form of more practically oriented controllers characterized by application simplicity, acceptable performance, and scalability with respect to a number of trailers present in a vehicle (see the comments in [31, 36]).

Motivated by the above arguments, the author presents a highly scalable nonlinear cascaded-like control approach to the PF problem for the nSNT vehicles. A novelty of the proposed concept comes from a combination of two components. The first one is a cascade-like control structure which leads to a modular and highly scalable state-feedback controller, which is relatively simple in implementation. Scalability makes a structure and complexity of the new control law independent on the number of trailers attached in a vehicle. Although utilization of the cascaded-like control paradigm into N-trailers is not a completely new concept (it has been independently developed and presented for the backward pushing task in [36, 37], for the trajectory-tracking task e.g. in [14], and for set-point control in [17, 32]), it is applied here for a first time in the context of the PF problem. The second component is the relatively new PF control law originally developed for unicycle kinematics in [39], which will be applied in the outer loop of a cascade. The main advantage of the approach presented in [39] (cf. also [15]) comes from a new way of treating the PF control problem which removes fundamental limitations of the well known and widely utilized PF control method introduced for unicycle-like robots in [47] (in this context see also [3, 22, 24, 38, 49, 51, 55]). By defining the so-called *segment-platooning* (S-P) reference paths, the newly proposed control law guarantees asymptotic following of both constant-curvature and varying-curvature S-P reference paths using either backward or forward motion strategy of a vehicle, with a guidance point fixed on the last trailer. In the paper it will be explained in what sense the new control

[☆]This work was supported by the statutory grant No. 93/194/13 DS-MK
Email address: maciej.michalek@put.poznan.pl (Maciej Marcin Michałek)

[1]Similar control concepts have found applications also in other areas of robotics, see e.g. [12, 28, 40].

law outperforms functionality of the PF controllers available in the literature for truly N-trailers with off-axle hitching.

This work is a substantial extension of conference paper [33].

2. Kinematics of N-trailer vehicles

The N-trailer (Fig. 1) comprises of a differentially driven tractor (segment number 0) and arbitrary number of N trailers of lengths $L_i > 0$, $i = 1, \ldots, N$, interconnected in a chain by passive rotary joints. Location of the ith vehicle joint is determined with respect to the $(i-1)$st segment by the hitching offset L_{hi}. We restrict our attention to the N-trailers characterized by ($i, j \in \{1, \ldots, N\}$):

A1. $L_{hi} > 0$ or $L_{hi} < 0$ with $|L_{hi}| < L_i$ in the second case,

A2. sign-homogeneous hitching: $\mathrm{sgn}(L_{hi}) = \mathrm{sgn}(L_{hj})$,

where $L_{hi} > 0$ if the ith joint is located *behind* the wheel-axle of a preceding segment (Fig. 1), and $L_{hi} < 0$ in the opposite case.

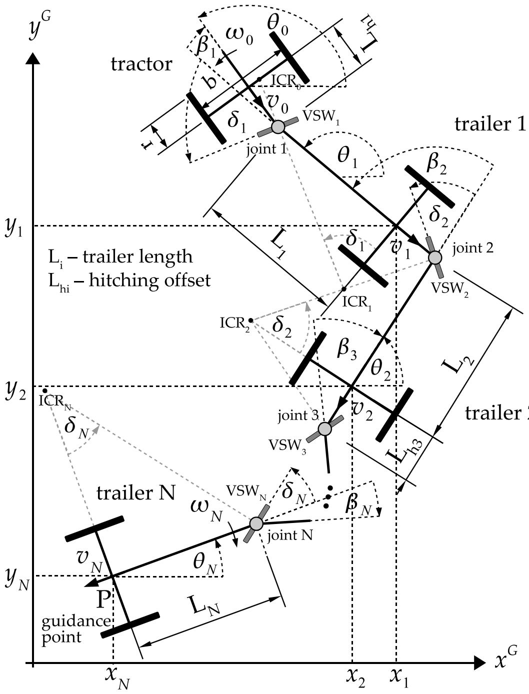

Figure 1: Kinematic structure of the N-trailer vehicle with definition of configuration variables and control inputs; the instantaneous centers of rotation (ICR) and virtual steering wheels (VSW) have been denoted for particular segments

Assumption A1 restricts the set of considered N-trailers to the nSNT kinematics. Although A1 excludes on-axle hitching, the most practical constructions of N-trailer robots equipped with single-axle trailers possess solely off-axle hitches (see e.g. [14, 26, 27, 36]). On the other hand, nSNT kinematics with $N > 1$ do not belong to the differentially flat systems, see [45], thus generally a control design problem cannot be solved in this case by the use of a chained-form transformation willingly applied into N-trailers with on-axle hitching. The lengths of negative hitching offsets have been delimited in A1 to the practical range. Assumption A2 is necessary to ensure stability of the vehicle chain in a closed-loop control system proposed in the sequel (see Section 4). A2 restricts the set of admissible nSNT constructions to those, in which all the joints are mounted either behind or in front of the preceding wheel axles. In a first view it may seem substantially limiting, however in practical constructions of N-trailer vehicles, and especially N-trailer robots, combination of sign-heterogeneous hitches appears very rarely, see e.g. [14, 16, 26, 37, 54].

Configuration vector of the N-trailer vehicle

$$\boldsymbol{q} \triangleq [\beta_1 \ \ldots \ \beta_N \ \theta_N \ x_N \ y_N]^\top = \left[\boldsymbol{\beta}^\top \ \boldsymbol{q}_N^\top\right]^\top \tag{1}$$

consists of a vector of joint angles $\boldsymbol{\beta} = [\beta_1 \ \ldots \ \beta_N]^\top \in \mathbb{T}^N$ and posture vector $\boldsymbol{q}_N = [\theta_N \ x_N \ y_N]^\top \in \mathbb{R}^3$ of the last-trailer (*guidance segment*). The only active segment is a tractor with control input $\boldsymbol{u}_0 = [\omega_0 \ v_0]^\top \in \mathbb{R}^2$, where ω_0 and v_0 are the angular and longitudinal tractor velocities, respectively (cf. Fig. 1). Under the rolling-without-skidding assumption one can treat any ith segment of the N-trailer as unicycle kinematics[2]:

$$\dot{\theta}_i = \omega_i, \quad \dot{x}_i = v_i \mathrm{c}\theta_i, \quad \dot{y}_i = v_i \mathrm{s}\theta_i \tag{2}$$

with virtual input $\boldsymbol{u}_i = [\omega_i \ v_i]^\top \in \mathbb{R}^2$ where ω_i and v_i are the angular and longitudinal velocities of the ith segment, respectively. Using basic velocity-geometry arguments it can be shown that for $i = 1, \ldots, N$ holds

$$\boldsymbol{u}_i = \boldsymbol{J}_i(\beta_i)\boldsymbol{u}_{i-1}, \qquad \boldsymbol{J}_i(\beta_i) = \begin{bmatrix} -\frac{L_{hi}}{L_i}\mathrm{c}\beta_i & \frac{1}{L_i}\mathrm{s}\beta_i \\ L_{hi}\,\mathrm{s}\beta_i & \mathrm{c}\beta_i \end{bmatrix}, \tag{3}$$

where $\boldsymbol{J}_i(\beta_i)$ is the transformation matrix. Since $\boldsymbol{J}_i(\beta_i)$ is always invertible under assumption A1, one can write:

$$\boldsymbol{u}_{i-1} = \boldsymbol{J}_i^{-1}(\beta_i)\boldsymbol{u}_i, \qquad \boldsymbol{J}_i^{-1}(\beta_i) = \begin{bmatrix} \frac{-L_i}{L_{hi}}\mathrm{c}\beta_i & \frac{1}{L_{hi}}\mathrm{s}\beta_i \\ L_i\,\mathrm{s}\beta_i & \mathrm{c}\beta_i \end{bmatrix}. \tag{4}$$

The joint-angle equation $\beta_i \triangleq \theta_{i-1} - \theta_i$ together with its time-derivative $\dot{\beta}_i = \omega_{i-1} - \omega_i$ complete the set of basic equations of the N-trailer kinematics, which can be combined together obtaining the following drift-free system (see [32, 34]):

$$\dot{\boldsymbol{q}} = \begin{bmatrix} \dot{\boldsymbol{\beta}} \\ \dot{\boldsymbol{q}}_N \end{bmatrix} = \begin{bmatrix} \boldsymbol{S}_\beta(\boldsymbol{\beta}) \\ \boldsymbol{S}_N(\boldsymbol{\beta}, \boldsymbol{q}_N) \end{bmatrix} \boldsymbol{u}_0, \tag{5}$$

where

$$\boldsymbol{S}_\beta = \begin{bmatrix} \boldsymbol{c}^\top \boldsymbol{\Gamma}_1(\beta_1) \\ \boldsymbol{c}^\top \boldsymbol{\Gamma}_2(\beta_2)\boldsymbol{J}_1(\beta_1) \\ \vdots \\ \boldsymbol{c}^\top \boldsymbol{\Gamma}_N(\beta_N) \prod_{j=N-1}^{1} \boldsymbol{J}_j(\beta_j) \end{bmatrix}, \quad \boldsymbol{S}_N = \begin{bmatrix} \boldsymbol{c}^\top \prod_{j=N}^{1} \boldsymbol{J}_j(\beta_j) \\ \boldsymbol{d}^\top \prod_{j=N}^{1} \boldsymbol{J}_j(\beta_j)\mathrm{c}\theta_N \\ \boldsymbol{d}^\top \prod_{j=N}^{1} \boldsymbol{J}_j(\beta_j)\mathrm{s}\theta_N \end{bmatrix} \tag{6}$$

and $\boldsymbol{\Gamma}_i(\beta_i) \triangleq \boldsymbol{I} - \boldsymbol{J}_i(\beta_i)$, $\boldsymbol{I} \in \mathbb{R}^{2\times 2}$ is a unit matrix, $\boldsymbol{c}^\top \triangleq [1 \ 0]$, $\boldsymbol{d}^\top \triangleq [0 \ 1]$.

3. Reference signals and control problem formulation

3.1. Definition of reference paths and reference joint angles

According to Fig. 1, the last trailer (guidance segment) is by definition distinguished in the context of a motion task. Let us define reference signals for the guidance segment by following the concept presented in [39]. The reference positional path on a motion plane can be defined by equation

$$F(x, y) \triangleq \sigma f(x, y) = 0, \qquad \sigma \in \{-1, +1\}, \tag{7}$$

[2] For compactness we will use the notation: $\mathrm{c}\alpha \equiv \cos\alpha$, $\mathrm{s}\alpha \equiv \sin\alpha$.

where σ is a binary decision factor (design parameter), the meaning of which will be clarified in the sequel. According to [39], one assumes that function $F(x,y)$ is well defined for $(x,y) \in \mathcal{D} \subset \mathbb{R}^2$, i.e.: $F(x,y)$ is bounded and at least twice differentiable ensuring existence of partial derivatives $F_x(x,y) \triangleq \partial F(x,y)/\partial x$, $F_y(x,y) \triangleq \partial F(x,y)/\partial y$, $F_{z_1 z_2}(x,y) \triangleq \partial^2 F(x,y)/\partial z_1 \partial z_2$, $z_1, z_2 \in \{x,y\}$, and gradient $\nabla F(x,y) = \left[F_x(x,y)\ F_y(x,y)\right]$ is non-zero: $\|\nabla F(x,y)\| > 0$ for $(x,y) \in \mathcal{D}$. Reference orientation

$$\theta_d(x,y) \triangleq \operatorname{Atan2c}\left(-F_x(x,y), F_y(x,y)\right) \in \mathbb{R}, \tag{8}$$

determines tangent direction to reference path (7) at point (x,y), where $\operatorname{Atan2c}(\cdot,\cdot): \mathbb{R}\times\mathbb{R} \mapsto \mathbb{R}$ is a continuous version of the four-quadrant function $\operatorname{Atan2}(\cdot,\cdot): \mathbb{R}\times\mathbb{R} \mapsto (-\pi,\pi]$ introduced to preserve continuity of orientation error in (10) (cf. Appendix A). Decision factor σ introduced in (7), and included in partial derivatives F_x and F_y, determines a desired quadrant for reference orientation $\theta_d(x,y)$ along the positional path. Formulas (7) and (8) determine a feasible reference path for unicycle kinematics respecting nonholonomic constraints imposed by (2)[3].

Since the last trailer has been selected as a guidance segment, posture $\boldsymbol{q}_N$ can be treated as a generic output of system (5)

$$\boldsymbol{y} \triangleq \boldsymbol{q}_N = \left[\boldsymbol{0}_{3\times N} \quad \boldsymbol{I}_{3\times 3}\right]\boldsymbol{q} = \boldsymbol{C}\boldsymbol{q}. \tag{9}$$

As a consequence, the path-following error will be defined with respect to the generic output $\boldsymbol{q}_N$ as follows:

$$\boldsymbol{e}(\boldsymbol{q}_N) \triangleq \begin{bmatrix} F(\boldsymbol{q}_N) \\ e_\theta(\boldsymbol{q}_N) \end{bmatrix} \triangleq \begin{bmatrix} \sigma f(x_N, y_N) \\ \theta_N - \theta_d(x_N, y_N) \end{bmatrix} \in \mathbb{R}^2, \tag{10}$$

where x_N, y_N are position coordinates of guidance point P (cf. Fig. 1). Component $F(\boldsymbol{q}_N)$ in definition (10) can be treated as a *signed distance value* (see [39]) determined between guidance point P and a reference path, since $F(\boldsymbol{q}_N) = 0$ only if P is exactly on a reference path (however in general, $F(\boldsymbol{q}_N)$ is not the Euclidean distance). Component $e_\theta(\boldsymbol{q}_N)$ is the orientation error evaluated at $\boldsymbol{q}_N$. Evaluation of the PF error (10) at any posture $\boldsymbol{q}_N$ does not require determination of the shortest distance to a reference path as it was needed in the classical approach to the PF problem introduced in [47]. This fact has substantial practical meaning, because determination of the shortest distance to a path of a general shape is the most difficult issue and limiting factor in practical applications of classical PF controllers.

Remark 1. *Since a reference path defined by (7)-(8) is feasible for unicycle kinematics, one may assume that there exist some nominal velocity functions Φ^*_ω, Φ^*_v which guarantee perfect guidance of the unicycle along the reference path with a prescribed longitudinal velocity determined by Φ^*_v. In other words, there exist feedforward velocities $\omega_N = \Phi^*_\omega, v_N = \Phi^*_v$ which applied into (2) with $i := N$ ensure that $\boldsymbol{e}(\boldsymbol{q}_N(t)) = \boldsymbol{0}$ for all $t \geq 0$ if $\boldsymbol{q}_N(0)$ is exactly on the path ('perfect output tracking' case). Functions Φ^*_ω, Φ^*_v will be called hereafter the* nominal guiding velocities.

Generic output (9) and PF error (10) strictly refer to the guidance segment only. For the purpose of stability analysis presented in Section 4.3 let us complement a set of reference signals with reference joint-angles β_{di}, $i = 1,\ldots,N$, which are compatible with the reference path. Assume then, that for a given reference path described by (7)-(8) there exist unique reference functions

$$\boldsymbol{\beta}_d(t) = [\beta_{d1}(t)\ldots\beta_{dN}(t)]^\top \in \left(-\frac{\pi}{2}, \frac{\pi}{2}\right)^N \tag{11}$$

which determine desired evolution of the vehicle joint angles for the case of 'perfect output tracking' (cf. Remark 1). By combination of joint-angle dynamics from (5) with iteratively applied formula (4) it can be found that reference functions (11) shall satisfy the following differential equation

$$\dot{\boldsymbol{\beta}}_d = \boldsymbol{S}_\beta(\boldsymbol{\beta}_d)\prod_{j=1}^{N}\boldsymbol{J}_j^{-1}(\beta_{dj})\boldsymbol{\Phi}^*, \quad \boldsymbol{\Phi}^* = [\Phi^*_\omega\ \Phi^*_v]^\top, \tag{12}$$

where $\boldsymbol{\Phi}^*$ is the nominal guiding velocity. It is well known that for the constant-curvature reference paths (circular and rectilinear ones) the reference functions $\beta_{di}(t) = \beta_{di} = \text{const}\ \forall i$, and for the rectilinear paths $\boldsymbol{\beta}_d = \boldsymbol{0}$ (see [11, 35]). In the case of varying-curvature reference paths the nominal guiding velocity $\boldsymbol{\Phi}^*$ is non-constant implying that $\boldsymbol{\beta}_d(t)$ is a time-varying 'steady-state' solution of (12). Finding analytical forms of functions (11) in the latter case is a non-trivial task (if at all possible), because nSNT kinematics is not differentially flat for $N > 1$ (cf. [45]). However, it will be shown in the sequel that knowledge about explicit analytical forms of functions (11) is not needed in our case, because angles $\boldsymbol{\beta}_d(t)$ will not be used in definition of the cascaded-like controller proposed in the paper.

3.2. Segment-platooning (S-P) reference paths

From a set of all possible constant- and varying-curvature reference paths, with reference joint angles (11) being a solution of (12), let us distinguish a subset of the so-called *segment-platooning* (S-P) reference paths, along which

$$\forall\, t \geq 0 \quad v_{di-1}(t)\cdot v_{di}(t) > 0, \qquad i = 1,\ldots,N, \tag{13}$$

where $v_{di}(t)$ and $v_{di-1}(t)$ denote the reference longitudinal velocities of, respectively, the ith and $(i-1)$st vehicle segments along the reference path resulting from relation

$$\begin{bmatrix} \omega_{di} \\ v_{di} \end{bmatrix} \overset{(3)}{=} \boldsymbol{J}_i(\beta_{di})\begin{bmatrix} \omega_{di-1} \\ v_{di-1} \end{bmatrix} \overset{(4)}{=} \prod_{j=i+1}^{N}\boldsymbol{J}_j^{-1}(\beta_{dj})\boldsymbol{\Phi}^*, \tag{14}$$

where $\boldsymbol{\Phi}^* = [\Phi^*_\omega\ \Phi^*_v]^\top$ denotes the nominal guiding velocity, and $[\omega_{dN}\ v_{dN}]^\top \equiv [\Phi^*_\omega\ \Phi^*_v]^\top$. Condition (13) means that the reference longitudinal velocities of every two neighboring vehicle segments are non-zero and have the same signs along the reference path (all segments persistently move either backward or forward – segment-platooning persistently exciting reference motion). It can be shown (see Appendix B) that satisfaction of (13) for reference joint angles (11) is equivalent to geometrical condition

$$\forall\, t \geq 0 \quad \tan\delta_{di}(t)\tan\beta_{di}(t) + 1 > 0, \qquad i = 1,\ldots,N, \tag{15}$$

where $\delta_{di}(t)$ denotes a steering angle of the ith virtual steering wheel along a reference path[4], while $\tan\delta_{di}(t) = L_i\,\kappa_{di}(t)$ with $\kappa_{di}(t) = \omega_{di}(t)/v_{di}(t)$ is a reference motion-curvature of the ith vehicle segment along a reference path (see Fig. 1). Most practically useful paths satisfy (13). In particular:

[3] In spite of technical modifications resulting from inclusion of binary factor σ in (7) and from using $\operatorname{Atan2c}(.,.)$ in (8), the above definition of a reference path conceptually corresponds to the original formulation presented in [39].

[4] The concept of virtual steering wheels (VSW) has been introduced by Altafini in [4]; VSW are denoted in Fig. 1 together with angles δ_i for exemplary motion conditions.

I. Rectilinear paths always satisfy (13) because in this case $\beta_{di} = \delta_{di} = 0$ for all $i - 1, \ldots, N$, and (15) is met $\forall\, t \geq 0$.

II. For circular paths, it can be shown that (see Appendix B) $v_{di-1} = v_{di} \cdot \rho_i$, where $\rho_i = (L_i + L_{hi}\mathrm{c}\beta_{di})/(L_i\mathrm{c}\beta_{di} + L_{hi})$. Thus (13) is satisfied if only $\rho_i > 0$, which in turn holds if:

   a) $(L_{hi} > 0) \wedge (|\beta_{di}| < \pi/2)$ for $i = 1, \ldots, N$, which is met for reference angles (11) under assumption A1,

   b) $(L_{hi} < 0) \wedge (|L_{hi}| < L_i) \wedge (\beta_{di} \in (-\gamma_i, \gamma_i))$ where $\gamma_i = \arccos(|L_{hi}|/L_i))$ for $i = 1, \ldots, N$; this case is compatible with assumption A1 but confines the admissible reference joint angles to the subset of (11) because $\gamma_i < \pi/2$ if only $L_{hi} \neq 0$.

III. For curvature-varying paths, satisfaction of (13) generally holds for sufficiently smooth paths (without cusps), along which angles $\beta_{di}(t)$ and $\delta_{di}(t)$ either have the same signs or at least one of them is sufficiently small (to meet (15)) when they have opposite signs. In general, it is difficult to say a priori which exactly varying-curvature paths satisfy (13). However for a particular considered reference path determined by (7)-(8), satisfaction of (13) can be easily checked before the vehicle motion (off-line) by solving numerically equation (12), and next by using transformation (14) for corresponding guiding velocity $\boldsymbol{\Phi}^*$ (see Section 4.3 and plots in Fig. 3).

From now on, the S-P reference paths will be of our particular interest. It will be shown in Section 4.3 that desirable behavior of the vehicle chain (in the sense defined by (17)) can be guaranteed for the reference paths which are of the S-P type.

3.3. Control problem statement

Having defined the reference signals, let us state the path-following control (PFC) problem.

Definition 1 (PFC Problem). *For kinematics (5), satisfying assumptions A1- A2, find a feedback control law $\boldsymbol{u}_0(\boldsymbol{\beta}, \boldsymbol{e}(\boldsymbol{q}_N), \cdot)$ which for the reference paths represented by (7)-(8) and (11) guarantees convergence of PF errors*

$$\lim_{t\to\infty} F(\boldsymbol{q}_N(t)) = 0, \quad \lim_{t\to\infty} e_\theta(\boldsymbol{q}_N(t)) = 2\eta\pi,\ \eta \in \mathbb{Z}, \tag{16}$$

entailing asymptotic stability of joint-angle error

$$\tilde{\boldsymbol{\beta}} \triangleq \boldsymbol{\beta}_d - \boldsymbol{\beta} \quad \textit{in the sense:} \quad \lim_{t\to\infty} \tilde{\boldsymbol{\beta}}(t) = \mathbf{0}. \tag{17}$$

Definition 1 states the PF task as an input-output control problem, where the generic output (9) should be stabilized around a reference path, while $\boldsymbol{\beta}$-part of kinematics (5) is treated as internal dynamics which shall be stabilized at $\boldsymbol{\beta}_d$. Such a prioritization of a motion task has strong practical justification in the field of long articulated vehicles and has been treated in the literature [9].

4. Cascaded-like control law and the main result

4.1. Derivation of a cascade-like control structure

Under assumption A1 one can utilize propagation formula (4), which applied iteratively for $i = 1, \ldots, N$ yields

$$\boldsymbol{u}_0(\boldsymbol{\beta}) = \prod_{j=1}^{N} \boldsymbol{J}_j^{-1}(\beta_j)\boldsymbol{u}_N. \tag{18}$$

Equation (18) determines how the guidance-segment velocity $\boldsymbol{u}_N = [\omega_N\ v_N]^\top$ may be forced by the tractor input $\boldsymbol{u}_0$. Since (18) is a purely algebraic mapping which depends only on the current joint-angles $\boldsymbol{\beta}$, velocities of the last trailer can be instantaneously forced with the tractor control inputs. Equation (18) defines in fact a velocity transformation with feedback from angles $\boldsymbol{\beta}(t)$, where $\boldsymbol{u}_N$ and $\boldsymbol{u}_0$ can be treated, respectively, as an input and an output of the transformation.

Consider the guidance segment as the unicycle with virtual control input $\boldsymbol{u}_N$ (cf. (2)). Suppose that some feedback control function is given

$$\boldsymbol{\Phi}(\boldsymbol{e}, \cdot) = \begin{bmatrix}\Phi_\omega(\boldsymbol{e}, \cdot) & \Phi_v(\boldsymbol{e}, \cdot)\end{bmatrix}^\top \in \mathbb{R}^2, \tag{19}$$

which, when directly applied into the unicycle input, ensures satisfaction of convergence conditions (16) for the reference path determined by (7)-(8). As a consequence, (19) represents the PF controller devised for unicycle kinematics; a particular form of function $\boldsymbol{\Phi}(\boldsymbol{e}, \cdot)$ will be given in Section 4.2. The idea is to use (18) and force $\boldsymbol{u}_N = \boldsymbol{\Phi}(\boldsymbol{e}, \cdot)$ by taking

$$\boldsymbol{u}_0(\boldsymbol{\beta}, \boldsymbol{\Phi}) \triangleq \prod_{j=1}^{N} \boldsymbol{J}_j^{-1}(\beta_j)\boldsymbol{\Phi}(\boldsymbol{e}, \cdot). \tag{20}$$

Equation (20) represents the cascade connection of the inner-loop transformation defined by (18) and the outer-loop PF controller (19) devised for unicycle kinematics with feedback from error (10).

4.2. Outer-loop controller

In general, control function (19) can be defined in different ways – exemplary propositions of PF controllers for unicycle kinematics can be found in [3, 22, 24, 38, 47, 51]. In our case, one proposes to apply the PF control law originally presented in [39], which does not require determination of the instantaneous shortest distance to a reference path (in contrast to the classical approach introduced in [47]). This property is practically important, since finding the shortest distance to a path of a general shape may be difficult and computationally costly. Moreover, its unique determination requires that the initial position of a vehicle is constrained to a vicinity around a reference path, a size of which is smaller than a doubled absolute value of the smallest reference curvature-radius along the path. Control law proposed in [39] is free of the mentioned limitations.

Following [39], the outer-loop controller (19) can be defined as follows[5]

$$\boldsymbol{\Phi}(\boldsymbol{e}, v_d) \triangleq \begin{bmatrix}\Phi_\omega(\boldsymbol{e}, v_d) \\ \Phi_v(v_d)\end{bmatrix}, \tag{21}$$

with

$$\begin{aligned}\Phi_\omega(\boldsymbol{e}, v_d) \triangleq &-k_1 \|\nabla F(\boldsymbol{q}_N)\| \frac{k_2\, \Phi_v(v_d)\, F(\boldsymbol{q}_N)}{\sqrt{1 + F^2(\boldsymbol{q}_N)}} \\ &- k_1 |\Phi_v(v_d)| \left[F_x(\boldsymbol{q}_N)\mathrm{c}\theta_N + F_y(\boldsymbol{q}_N)\mathrm{s}\theta_N\right] + \dot{\theta}_d,\end{aligned} \tag{22}$$

$$\Phi_v(v_d) \triangleq v_d = \text{const}, \quad v_d \neq 0, \tag{23}$$

where $F_x(\boldsymbol{q}_N) \equiv F_x(x_N, y_N)$, $F_y(\boldsymbol{q}_N) \equiv F_y(x_N, y_N)$, coefficients

$$k_1 > 0, \quad k_2 \in (0, 1] \tag{24}$$

[5] Definition (22)-(23) is equivalent to the original formulation proposed in [39] for the special (but most common) case where $\Phi_v^* = v_d = \text{const}$.

are the design parameters, and

$$\dot{\theta}_d = \Phi_v(v_d)\frac{F_1(\boldsymbol{q}_N)\mathrm{c}\theta_N + F_2(\boldsymbol{q}_N)\mathrm{s}\theta_N}{\|\nabla F(\boldsymbol{q}_N)\|^2}, \tag{25}$$

$$F_1(\boldsymbol{q}_N) = F_x(\boldsymbol{q}_N)F_{xy}(\boldsymbol{q}_N) - F_y(\boldsymbol{q}_N)F_{xx}(\boldsymbol{q}_N), \tag{26}$$

$$F_2(\boldsymbol{q}_N) = F_x(\boldsymbol{q}_N)F_{yy}(\boldsymbol{q}_N) - F_y(\boldsymbol{q}_N)F_{xy}(\boldsymbol{q}_N). \tag{27}$$

For the purpose of further considerations and in order to indicate original properties of the PF controller (22)-(23) when it is directly applied into unicycle kinematics, let us recall the main result of work [39] in the form of a lemma.

Lemma 1 (upon [39], Th. 2). *For the reference paths determined by (7)-(8), direct application of control functions (22)-(23) into unicycle kinematics (2) with $i = N$ by taking $\omega_N := \Phi_\omega(\boldsymbol{e}, v_d)$ and $v_N := \Phi_v(v_d)$ guarantees convergence determined by (16) for any initial condition $\boldsymbol{e}(\boldsymbol{q}_N(0))$ with $(x_N(0), y_N(0)) \in \mathcal{D}$, outside the set of unstable equilibria: $\{F(\boldsymbol{q}_N) = 0, e_\theta = (2\eta + 1)\pi)|\, \eta \in \mathbb{Z}\}$.*

According to above result, it is not difficult to check that along the reference path $\boldsymbol{\Phi}(\boldsymbol{0}, v_d) = \boldsymbol{\Phi}^* = [\Phi^*_\omega\ \Phi^*_v]^\top$ with nominal guiding velocities

$$\Phi^*_\omega = \Phi_\omega(\boldsymbol{0}, v_d) = v_d\frac{F_1(\boldsymbol{q}_N)F_y(\boldsymbol{q}_N) - F_2(\boldsymbol{q}_N)F_x(\boldsymbol{q}_N)}{\|\nabla F(\boldsymbol{q}_N)\|^2}, \qquad \Phi^*_v = v_d. \tag{28}$$

4.3. Main result

Proposition 1. *Cascaded-like state-feedback PF controller*

$$\boldsymbol{u}_0(\boldsymbol{\beta}, \boldsymbol{\Phi}(\boldsymbol{e}, v_d)) \triangleq \prod_{j=1}^{N} \boldsymbol{J}_j^{-1}(\beta_j)\boldsymbol{\Phi}(\boldsymbol{e}, v_d) \tag{29}$$

with $\boldsymbol{\Phi}(\boldsymbol{e}, v_d)$ defined by (21)-(23) solves PFC Problem for any initial condition $\boldsymbol{e}(\boldsymbol{q}_N(0))$ with $(x_N(0), y_N(0)) \in \mathcal{D}$ outside the set $\{F(\boldsymbol{q}_N) = 0, e_\theta = (2\eta + 1)\pi)|\, \eta \in \mathbb{Z}\}$ guaranteeing local asymptotic stability of point $\tilde{\boldsymbol{\beta}} = \boldsymbol{0}$ for the S-P reference paths under the following conditions:

- *c1. $sgn(v_d) = -sgn(L_{hi})$, $\forall\, i = 1, \ldots, N$,*
- *c2. $\forall\, t \geq 0$ $\|\boldsymbol{\Phi}^*(t)\| \leq \delta_1$ and $\left\|\dot{\boldsymbol{\Phi}}^*(t)\right\| \leq \delta_2$ with sufficiently small constants $\delta_1, \delta_2 > 0$ for the case of varying-curvature reference paths.*

It will be shown in the proof of Proposition 1 that conditions *c1* and *c2* are required solely to ensure asymptotic stability of joint-angle error (17) – they do not affect convergence (16) for PF error (10). Under restriction *c1*, the guidance segment can follow a reference path either backward if all L_{hi} are positive, or forward if all L_{hi} are negative, keeping location of the guidance point on the last trailer. Since velocity v_d is selected by a designer, it is always possible to make a selection which satisfies *c1*. Furthermore, the upper bounds imposed by condition *c2* on the norm of nominal guiding velocity $\boldsymbol{\Phi}^*$ and its time-variability concern only the varying-curvature reference paths. Condition *c2* means that Proposition 1 admits the S-P varying-curvature reference paths which are sufficiently slow and smooth.

Figure 2 presents a block scheme which clarifies the proposed PF cascaded-like control structure for the nSNT robots. Reference path is uniquely determined by the form of function $F(x, y)$. The outer-loop PF controller is responsible for computing the instantaneous control function $\boldsymbol{\Phi}(\boldsymbol{e}, v_d)$ upon the current path-following error (10) and desired velocity v_d. Function $\boldsymbol{\Phi}(\boldsymbol{e}, v_d)$ determines instantaneous velocities, which would guide the last trailer toward (and then along) the reference path if $\boldsymbol{\Phi}(\boldsymbol{e}, v_d)$ is directly forced on virtual input $\boldsymbol{u}_N$. The role of the inner-loop transformation is to on-line recompute velocity $\boldsymbol{\Phi}(\boldsymbol{e}, v_d)$ into instantaneous control input $\boldsymbol{u}_0$ for the tractor segment upon the current values of vehicle joint angles $\boldsymbol{\beta}$. Application of input $\boldsymbol{u}_0(\boldsymbol{\beta}, \boldsymbol{\Phi})$ into the tractor makes the last trailer move in a way as it would be directly driven by function $\boldsymbol{\Phi}(\boldsymbol{e}, v_d)$. Worth noting that the control structure in Fig. 2 remains valid regardless a number of trailers present in a vehicle chain. A change of the trailers number affects only a number of matrix-multiplications used in transformation (29). As a consequence, the proposed controller is highly scalable, and reconfiguration of the control program for different numbers of trailers can be easily automated.

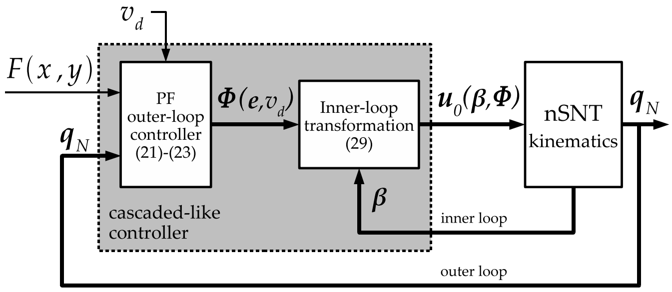

Figure 2: Block scheme of the proposed PF controller for nSNT robots

Proof of Proposition 1. First, let us examine closed-loop behavior of the guidance segment. In the closed-loop system

$$\boldsymbol{u}_N \overset{(3,29)}{=} \prod_{j=N}^{1} \boldsymbol{J}_j(\beta_j) \prod_{j=1}^{N} \boldsymbol{J}_j^{-1}(\beta_j)\boldsymbol{\Phi}(\boldsymbol{e}, v_d) = \boldsymbol{\Phi}(\boldsymbol{e}, v_d).$$

Hence, application of control law (29) makes the guidance segment move in a way as it would be directly controlled by the outer-loop function $\boldsymbol{\Phi}(\boldsymbol{e}, v_d)$. Now, one can apply Lemma 1 to conclude that control law (29) guarantees satisfaction of (16) for initial conditions $\boldsymbol{e}(\boldsymbol{q}_N(0))$ constrained to the domain prescribed in Proposition 1 (outer-loop dynamics inherit properties of the PF control loop proposed in [39]). The above conclusion is valid for both constant-curvature as well as varying-curvature reference paths.

Second, let us show boundedness of control function (29). Claiming the boundedness of the PF control law proposed in [39], one infers

$$\forall\, t \geq 0 \quad \|\boldsymbol{\Phi}(\boldsymbol{e}(\boldsymbol{q}_N(t)), v_d)\| \leq \phi_{\max} < \infty, \tag{30}$$

and in turn

$$\|\boldsymbol{u}_0(\boldsymbol{\beta}, \boldsymbol{\Phi})\| \overset{(29)}{=} \left\| \prod_{j=1}^{N} \boldsymbol{J}_j^{-1}(\beta_j)\boldsymbol{\Phi}(\boldsymbol{e}, v_d) \right\| \leq \prod_{j=1}^{N} M_j\phi_{\max} < \infty,$$

where the norm $M_j = \sqrt{\left(1 + L_j^2\mu_j^2\right)\mathrm{c}^2\beta_j + \left(\mu_j^2 + L_j^2\right)\mathrm{s}^2\beta_j}$, $\mu_j = 1/L_{hj}$, of matrix $\boldsymbol{J}_j^{-1}(\beta_j)$ is bounded under assumption A1.

Next, we shall consider stability of the joint-angles error dynamics in the closed-loop system. To this aim, let us provide some useful auxiliary relations which can be obtained by direct computations:

$$\boldsymbol{\Gamma}_i(\beta_{di}) \overset{(6)}{=} \boldsymbol{I} - \boldsymbol{J}_i(\beta_{di}), \tag{31}$$

$$\boldsymbol{\Gamma}_i(\beta_i) \overset{(17)}{=} \boldsymbol{\Gamma}_i(\beta_{di} - \tilde{\beta}_i) \overset{(6)}{=} \boldsymbol{I} - \boldsymbol{J}_i(\beta_{di})\boldsymbol{R}_{hi}(\tilde{\beta}_i), \tag{32}$$

$$\boldsymbol{J}_i^{-1}(\beta_i) \overset{(17)}{=} \boldsymbol{J}_i^{-1}(\beta_{di} - \tilde{\beta}_i) = \boldsymbol{J}_i^{-1}(\beta_{di})\boldsymbol{R}_i(\tilde{\beta}_i), \tag{33}$$

where

$$\boldsymbol{R}_{hi}(\tilde{\beta}_i) \triangleq \begin{bmatrix} c\tilde{\beta}_i & \frac{1}{L_{hi}}s\tilde{\beta}_i \\ -L_{hi}s\tilde{\beta}_i & c\tilde{\beta}_i \end{bmatrix}, \quad \boldsymbol{R}_i(\tilde{\beta}_i) \triangleq \begin{bmatrix} c\tilde{\beta}_i & \frac{1}{L_i}s\tilde{\beta}_i \\ -L_is\tilde{\beta}_i & c\tilde{\beta}_i \end{bmatrix},$$

and $\boldsymbol{R}_{hi}(0) = \boldsymbol{R}_i(0) = \boldsymbol{I}$. Define the outer-loop control difference

$$\tilde{\boldsymbol{\Phi}} \triangleq \boldsymbol{\Phi}^* - \boldsymbol{\Phi}(\boldsymbol{e}, v_d) \tag{34}$$

where $\boldsymbol{\Phi}^* = [\Phi_\omega^* \ \Phi_v^*]^\top = \boldsymbol{\Phi}(\boldsymbol{0}, v_d)$ with components resulting from (28). Taking a time-derivative of error $\tilde{\boldsymbol{\beta}}$ defined in (17), and then utilizing (5), (12), and (34) allows one to write the joint-error dynamics in the following form:

$$\dot{\tilde{\boldsymbol{\beta}}} = \boldsymbol{S}_\beta(\boldsymbol{\beta}_d)\prod_{j=1}^{N}\boldsymbol{J}_j^{-1}(\beta_{dj})\boldsymbol{\Phi}^* - \boldsymbol{S}_\beta(\boldsymbol{\beta}_d - \tilde{\boldsymbol{\beta}})\prod_{j=1}^{N}\boldsymbol{J}_j^{-1}(\beta_{dj} - \tilde{\beta}_j)(\boldsymbol{\Phi}^* - \tilde{\boldsymbol{\Phi}}). \tag{35}$$

It is clear that the pair $(\tilde{\boldsymbol{\beta}} = \boldsymbol{0}, \tilde{\boldsymbol{\Phi}} = \boldsymbol{0})$ is an equilibrium of dynamics (35). Recalling the form of matrix $\boldsymbol{S}_\beta$ (cf. (6)) and by utilizing formulas (31)-(33) one can obtain dynamics of the ith joint-angle error

$$\dot{\tilde{\beta}}_i = f_i(\tilde{\boldsymbol{\beta}}_{i,N}, \boldsymbol{\beta}_d, \boldsymbol{\Phi}^*) + g_i(\tilde{\boldsymbol{\beta}}_{i,N}, \boldsymbol{\beta}_d, \tilde{\boldsymbol{\Phi}}), \quad i = 1, \ldots, N, \tag{36}$$

where

$$\tilde{\boldsymbol{\beta}}_{i,N} \triangleq [\tilde{\beta}_i \ \tilde{\beta}_{i+1} \ \ldots \ \tilde{\beta}_N]^\top, \tag{37}$$

and

$$\begin{aligned} f_i = {} & \boldsymbol{c}^\top (\boldsymbol{I} - \boldsymbol{J}_i(\beta_{di}))\prod_{j=i}^{N}\boldsymbol{J}_j^{-1}(\beta_{dj})\boldsymbol{\Phi}^* \\ & - \boldsymbol{c}^\top \left(\boldsymbol{I} - \boldsymbol{J}_i(\beta_{di})\boldsymbol{R}_{hi}(\tilde{\beta}_i)\right)\prod_{j=i}^{N}\boldsymbol{J}_j^{-1}(\beta_{dj})\boldsymbol{R}_j(\tilde{\beta}_j)\boldsymbol{\Phi}^*, \end{aligned} \tag{38}$$

$$g_i = \boldsymbol{c}^\top \left(\boldsymbol{I} - \boldsymbol{J}_i(\beta_{di})\boldsymbol{R}_{hi}(\tilde{\beta}_i)\right)\prod_{j=i}^{N}\boldsymbol{J}_j^{-1}(\beta_{dj})\boldsymbol{R}_j(\tilde{\beta}_j)\tilde{\boldsymbol{\Phi}}. \tag{39}$$

Upon the forms of functions (38)-(39) one can recognize the upper-triangular structure of equation (35). For the purpose of stability analysis, let us linearize (35) at equilibrium $(\tilde{\boldsymbol{\beta}} = \boldsymbol{0}, \tilde{\boldsymbol{\Phi}} = \boldsymbol{0})$ treating $\tilde{\boldsymbol{\beta}}$ as a state, and $\tilde{\boldsymbol{\Phi}}$ as an input. We obtain:

$$\dot{\tilde{\boldsymbol{\beta}}} = \boldsymbol{A}(\boldsymbol{\beta}_d, \boldsymbol{\Phi}^*)\tilde{\boldsymbol{\beta}} + \boldsymbol{B}(\boldsymbol{\beta}_d)\tilde{\boldsymbol{\Phi}}, \tag{40}$$

with

$$\boldsymbol{A}(\boldsymbol{\beta}_d, \boldsymbol{\Phi}^*) = \begin{bmatrix} a_{11} & a_{12} & \ldots & a_{1N} \\ 0 & a_{22} & \ldots & a_{2N} \\ \vdots & \vdots & \ddots & \vdots \\ 0 & 0 & \ldots & a_{NN} \end{bmatrix}, \quad \boldsymbol{B}(\boldsymbol{\beta}_d) = \begin{bmatrix} \boldsymbol{b}_1^\top \\ \boldsymbol{b}_2^\top \\ \vdots \\ \boldsymbol{b}_N^\top \end{bmatrix}, \tag{41}$$

where diagonal elements of matrix $\boldsymbol{A}(\boldsymbol{\beta}_d, \boldsymbol{\Phi}^*)$ are

$$a_{ii} = \begin{bmatrix} \frac{L_is\beta_{di}}{L_{hi}} & \frac{c\beta_{di}}{L_{hi}} \end{bmatrix}\prod_{j=i+1}^{N}\boldsymbol{J}_j^{-1}(\beta_{dj})\boldsymbol{\Phi}^*, \quad i = 1, \ldots, N-1, \tag{42}$$

$$a_{NN} = \begin{bmatrix} \frac{L_Ns\beta_{dN}}{L_{hN}} & \frac{c\beta_{dN}}{L_{hN}} \end{bmatrix}\boldsymbol{\Phi}^*, \tag{43}$$

the non-zero off-diagonal elements take the form

$$a_{il} = \begin{bmatrix} 1 + \frac{L_ic\beta_{di}}{L_{hi}} \\ \frac{-s\beta_{di}}{L_{hi}} \end{bmatrix}^\top \prod_{j=i+1}^{l}\boldsymbol{J}_j^{-1}(\beta_{dj})\begin{bmatrix} 0 & \frac{1}{L_l} \\ -L_l & 0 \end{bmatrix}\prod_{j=l+1}^{N}\boldsymbol{J}_j^{-1}(\beta_{dj})\boldsymbol{\Phi}^* \tag{44}$$

for $i = 1, \ldots, N-1$, $l = i+1, \ldots, N$, and the ith row of $\boldsymbol{B}(\boldsymbol{\beta}_d)$ is

$$\boldsymbol{b}_i^\top = \begin{bmatrix} (1 + \frac{L_{hi}c\beta_{di}}{L_i}) & \frac{-s\beta_{di}}{L_i} \end{bmatrix}\prod_{j=i}^{N}\boldsymbol{J}_j^{-1}(\beta_{dj}), \quad i = 1, \ldots, N.$$

Linear system (40) locally approximates internal dynamics of the closed-loop system. Under the 'perfect output tracking' conditions, i.e. for $\boldsymbol{e}(\boldsymbol{q}_N) \equiv \boldsymbol{0}$ and $\tilde{\boldsymbol{\Phi}} \equiv \boldsymbol{0}$, system (40) takes the form

$$\dot{\tilde{\boldsymbol{\beta}}} = \boldsymbol{A}(\boldsymbol{\beta}_d, \boldsymbol{\Phi}^*)\tilde{\boldsymbol{\beta}} \tag{45}$$

and locally approximates zero-dynamics of the closed-loop system. Stability of dynamics (45) at $\tilde{\boldsymbol{\beta}} = \boldsymbol{0}$ results from properties of matrix $\boldsymbol{A}$. Since $\boldsymbol{A}(\boldsymbol{\beta}_d, \boldsymbol{\Phi}^*)$ has the upper-triangular structure, the eigenvalues $\lambda_i(\boldsymbol{A})$, $i = 1, \ldots, N$ are equal to its diagonal elements. Recalling (42)-(43) and (14) one can find

$$a_{ii} = \frac{v_{di-1}(t)}{L_{hi}} = \frac{\text{sgn}(v_{di-1}(t))\,|v_{di-1}(t)|}{L_{hi}}, \quad i = 1, \ldots, N.$$

For S-P reference paths we can utilize assumption (13), which together with condition *c1* allows us to write for $i = 1, \ldots, N$:

$$a_{ii} = \frac{\text{sgn}(v_d)\,|v_{di-1}(t)|}{L_{hi}} = \frac{-\,|v_{di-1}(t)|}{|L_{hi}|} \leq -\alpha, \tag{46}$$

where

$$\alpha = \min_{i\in\{1,\ldots,N\}}\left\{\inf_{t\geq 0}\left|\frac{v_{di-1}(t)}{L_{hi}}\right|\right\} > 0. \tag{47}$$

Hence, (46)-(47) indicate that all the eigenvalues of matrix $\boldsymbol{A}(\boldsymbol{\beta}_d, \boldsymbol{\Phi}^*)$ are real-negative for any S-P reference path.

For the constant-curvature S-P reference paths (rectilinear and circular ones) the reference angles (11), velocity $\boldsymbol{\Phi}^*$, and all reference velocities v_{di}, $i = 0, \ldots, N$, are constant (cf. (14)), thus matrix $\boldsymbol{A}(\boldsymbol{\beta}_d, \boldsymbol{\Phi}^*)$ becomes time-invariant. In this case, local exponential stability of zero-dynamics (45) at $\tilde{\boldsymbol{\beta}} = \boldsymbol{0}$ results directly from (46)-(47).

In the case of curvature-varying reference paths, the reference angles (11), velocity $\boldsymbol{\Phi}^*$, and reference velocities $v_{di}(t)$, $i = 0, \ldots, N$, are generally varying in time. As a consequence, $\boldsymbol{A}(\boldsymbol{\beta}_d(t), \boldsymbol{\Phi}^*(t)) = \boldsymbol{A}(t)$ and asymptotic stability analysis for LTV system (45) is more involving. In this case, one can utilize a result recalled in Appendix A in the form of Lemma 2, which provides sufficient stability conditions for LTV systems. Let us analyze satisfaction of all the conditions required by Lemma 2.

Recalling the form of matrix $\boldsymbol{A}(\boldsymbol{\beta}_d(t), \boldsymbol{\Phi}^*(t))$ in (41) and components (42)-(44) it is evident that $\left|a_{ij}(\boldsymbol{\beta}_d(t), \boldsymbol{\Phi}^*(t))\right| < \bar{a} < \infty$, $i, j \in \{1, \ldots, N\}$, for all $t \geq 0$ under assumption A1 and by using (30) for $\boldsymbol{\Phi}(\boldsymbol{0}, v_d) = \boldsymbol{\Phi}^*$. As a consequence,

$$\|\,\boldsymbol{A}(\boldsymbol{\beta}_d(t), \boldsymbol{\Phi}^*(t))\| < \bar{A} < \infty, \quad \forall\, t \geq 0.$$

Since (46)-(47) hold also for the varying-curvature S-P reference paths we have $\lambda_i(\boldsymbol{A}(\boldsymbol{\beta}_d(t), \boldsymbol{\Phi}^*(t))) \leq -\alpha$, $i = 1, \ldots, N$, and it remains to analyze time-variability of matrix $\boldsymbol{A}(\boldsymbol{\beta}_d(t), \boldsymbol{\Phi}^*(t))$. To this aim, one can write $\dot{a}_{ij}(\boldsymbol{\beta}_d(t), \boldsymbol{\Phi}^*(t)) = \boldsymbol{a}_{\beta ij}^\top\dot{\boldsymbol{\beta}}_d + \boldsymbol{a}_{\phi ij}^\top\dot{\boldsymbol{\Phi}}^*$,

$i, j \in \{1, \ldots, N\}$, where $\boldsymbol{a}_{\beta ij}^{\top} \triangleq \partial a_{ij}/\partial \boldsymbol{\beta}_d$ and $\boldsymbol{a}_{\phi ij}^{\top} \triangleq \partial a_{ij}/\partial \boldsymbol{\Phi}^*$. Under assumption A1 and using (30) one claims (cf. (42)-(44)):

$$\left\| \boldsymbol{a}_{\beta ij}^{\top} \right\| \le \delta_{\beta ij} < \infty, \quad \left\| \boldsymbol{a}_{\phi ij}^{\top} \right\| \le \delta_{\phi ij} < \infty. \tag{48}$$

Recalling (12) one can (conservatively) assess

$$\left\| \dot{\boldsymbol{\beta}}_d \right\| \le \left\| \boldsymbol{S}_{\beta}(\boldsymbol{\beta}_d) \prod_{j=1}^{N} \boldsymbol{J}_j^{-1}(\beta_{dj}) \right\| \|\boldsymbol{\Phi}^*\| \le \delta_{\beta} \|\boldsymbol{\Phi}^*\|, \tag{49}$$

where $0 < \delta_{\beta} < \infty$ under assumption A1 and due to the form of matrix (6). Now, under condition *c2* and according to (48)-(49) we can write

$$\forall\, t \ge 0 \quad \left| \dot{a}_{ij}(\boldsymbol{\beta}_d(t), \boldsymbol{\Phi}^*(t)) \right| \le \delta_{\beta ij}\, \delta_{\beta}\, \delta_1 + \delta_{\phi ij}\, \delta_2 < \infty,$$

and consequently (with $\|\cdot\|$ denoting a spectral norm, [50])

$$\begin{aligned} \forall\, t \ge 0 \quad \left\| \dot{\boldsymbol{A}}(\boldsymbol{\beta}_d(t), \boldsymbol{\Phi}^*(t)) \right\| &\le N \max_{i,j} \left| \dot{a}_{ij}(\boldsymbol{\beta}_d(t), \boldsymbol{\Phi}^*(t)) \right| \\ &\le N \left(\bar{\delta}_{\beta ij}\, \delta_{\beta}\, \delta_1 + \bar{\delta}_{\phi ij}\, \delta_2 \right), \end{aligned} \tag{50}$$

where $\bar{\delta}_{\beta ij} = \max_{i,j}(\delta_{\beta ij})$ and $\bar{\delta}_{\phi ij} = \max_{i,j}(\delta_{\phi ij})$. Now, the right-hand side of inequality (50) can be made small enough to satisfy (C.1) by providing sufficiently small constants δ_1 and δ_2 (as in condition *c2*), and consequently guaranteeing local exponential stability of (45) at $\tilde{\boldsymbol{\beta}} = \boldsymbol{0}$ in the case of varying-curvature reference paths. Worth noting that (50) is fairly conservative, because it expresses the sufficient but not necessary condition for stability of (45), see [56]. □

In order to validate theoretical forecasts formulated in Proposition 1, and formally considered in the Proof, two sets of simulation results have been presented in Fig. 3. The plots illustrate time evolution of path-following errors, joint-angle errors, and reference longitudinal velocities in two cases: for the constant-curvature (circular) path, and for the varying-curvature (elliptical) reference path. Reference joint angles (11) were computed by numerical integration of equation (12) substituting $\boldsymbol{\Phi}^* := [\dot{\theta}_d\ v_d]^{\top}$ and taking $\boldsymbol{\beta}_d(0) = \boldsymbol{0}$, while reference velocities $v_{di}(t)$ were computed upon[6] (14). The results have been obtained for the nS3T kinematics selecting $\boldsymbol{q}(0) = [\boldsymbol{0}_{3\times 1}\ 0\ -0.5\ 0]^{\top}$, and using the common parameters: $L_i = 0.25$ m, $L_{hi} = 0.04$ m, $i = 1, 2, 3$, $v_d = -0.3$ m/s, $\sigma = -1$, and $k_1 = 2$, $k_2 = 1$. Both reference paths have been defined by taking $f(x, y) := (x^2/A^2) + (y^2/B^2) - 1$ with $A = B = 1$ for the circular path, and $A = 2, B = 1$ for the elliptical one. Worth stressing that all the errors plotted in Fig. 3 asymptotically tend to zero both for constant-curvature as well as for varying-curvature reference path (see also [33]). The plots in the last column in Fig. 3 reveal that in both cases the reference paths are of S-P type, since all reference velocities $v_{di}(t)$ have a common sign compatible with $v_{d3} \equiv \Phi_v^* = v_d = -0.3$ m/s.

Remark 2. *According to work [39], factor σ in (7) determines only a sign of function $F(x, y)$ and, as a consequence, the quadrants in which reference orientation (8) is defined. However, it turns out that selection of $\sigma \in \mathbb{R} \setminus \{0\}$ (in contrast to the binary set introduced in (7)) allows rescaling function $F(x, y)$ and gradient $\nabla F(x, y)$, influencing in this way the convergence rate of PF error (10). In this context, component $F(\boldsymbol{q}_N)$ in (10) for $|\sigma| \ne 1$ shall be treated now as the* scaled signed distance value, *while $|\sigma|$ can be used as an additional design parameter, helping one shape transient states in the closed-loop system. Exemplary plot of surface $F(x, y) = \sigma f(x, y)$ for different values of factor σ has been presented in Fig. 4. It is evident that σ does not change a shape of the reference path (in this case the elliptical one), but it only affects values of $F(x, y)$ and its slope around the path.*

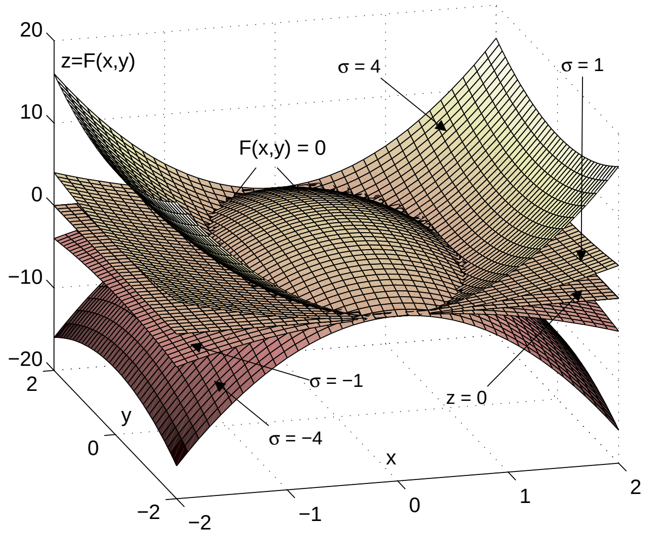

Figure 4: Surface $z = F(x, y) = \sigma f(x, y)$ with $f(x, y) = 0.25x^2 + y^2 - 1$ for different values of factor σ; intersection of the surface with plane $z = 0$ determines the elliptical reference path (cf. (7))

Fig. 5 illustrates the influence of $|\sigma|$ on vehicle motion character and on the convergence rate of PF errors for the el-

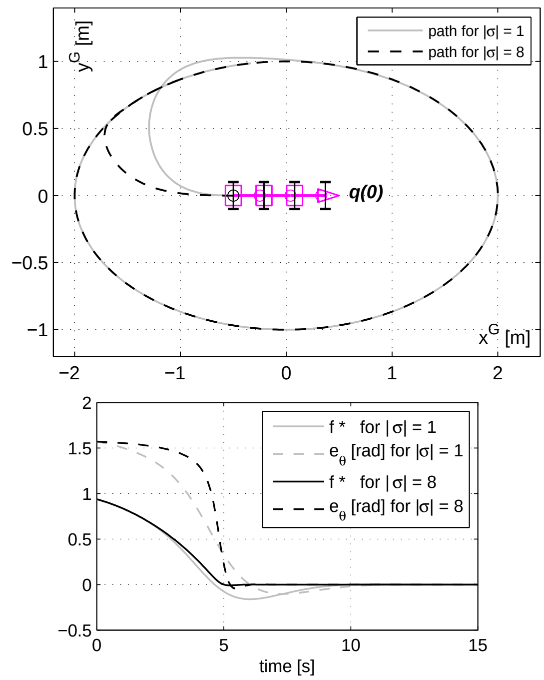

Figure 5: Comparison of paths drawn by the guidance point P and convergence rates of PF error components for two selected values of $|\sigma|$ in the case of elliptical reference path (the same initial vehicle configuration $\boldsymbol{q}(0)$ has been assumed for both cases)

[6] Since $\dot{\theta}_d(\boldsymbol{q}_N(t)) \to \Phi_{\omega}(\boldsymbol{0}, v_d)$ as $t \to \infty$, signals $v_{di}(t)$ computed numerically include transient components which are negligibly small after about 13 seconds in case of simulations shown in Fig. 3 (after this time $v_{di}(t)$ well corresponds to true reference velocities along the path).

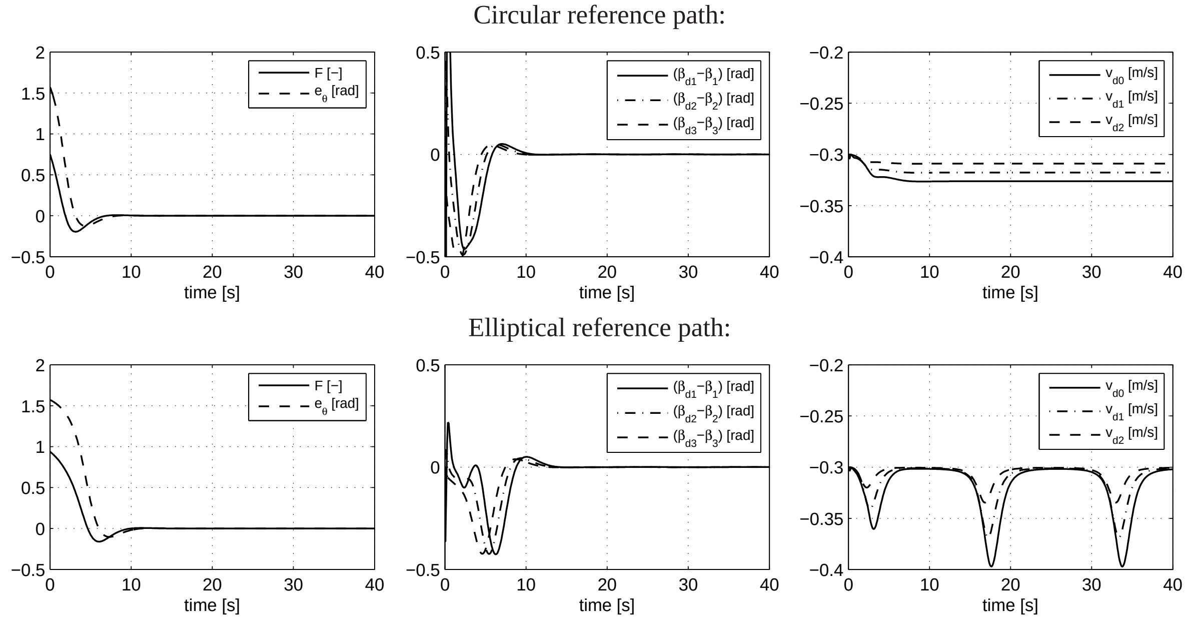

Figure 3: Time-evolution of path-following errors F, e_θ, joint-angle errors $\tilde{\beta}_i = \beta_{di} - \beta_i$, $i = 1, 2, 3$, and reference longitudinal velocities v_{di}, $i = 0, 1, 2$ for the constant-curvature (circular) and varying-curvature (elliptical) reference paths (velocities $v_{di}(t)$ have been numerically computed upon (14) and (12) for $\boldsymbol{\beta}_d(0) = \mathbf{0}$)

liptical reference path (instead of $F(\boldsymbol{q}_N(t))$, the time-plots of $f^*(\boldsymbol{q}_N(t)) \triangleq F(\boldsymbol{q}_N(t))/|\sigma|$ have been presented to ensure the same scale for both signals). It can be seen that by increasing a value of $|\sigma|$ one can speedup convergence of PF errors. A direct consequence of the higher convergence rate is less smooth motion of a vehicle when entering a reference path. Thus in practice, selection of $|\sigma|$ shall result from a compromise between expected convergence rate of PF errors and desired smoothness of vehicle motion within a transient stage.

4.4. *Comparison of the proposed controller with other methods*

Let us qualitatively compare the proposed method with alternative feedback-control approaches available in the literature. We will consider only comparable methods, i.e. those which are devoted to the PF motion task for truly N-trailers (admitting arbitrary number of trailers) equipped with off-axle hitches and fixed (non-steerable) wheel axles (nSNT or GNT vehicles[7]). The literature is very limited in this area, and to the author's best knowledge it is virtually represented by works [5, 6, 9, 10]. One shall note that the control task defined in [5, 6] is conceptually different when compared with a more classical approach to the PF problem presented in [9, 10] and in the current paper. In [5, 6], the task is not defined with respect to a single guidance segment, but concerns simultaneously all the vehicle segments which have to be kept as close to the reference path as possible in the average sense. This concept may be useful e.g. in the case where the whole N-trailer has to follow along a road of a limited width, while the classical approach is more appropriate to the problem of precise following a desired contour (path) by an implement located on the guidance segment. The table presented in Fig. 6 provides qualitative comparison of control laws with respect to ten selected features which are important from either theoretical or application perspective. It can be seen that all the considered control laws have some limitations, also with respect to values/signs of hitching offsets present in a vehicle chain. The 'ghost-vehicle' approach seems admit arbitrary hitching offsets, however it suffers from substantial complexity (low scalability) of controller equations, and was analyzed in [10] only for $N \leq 2$.

Especially beneficial properties of the cascaded-like controller have been highlighted in bold in the last column. Since the new control law does not utilize the linearization concept, it can be globally well defined if only a reference path is such that $\forall\,(x, y)\ \|\nabla F(x, y)\| > 0$ (in contrast to comparable controllers

Method → / **Feature ↓**	Reduced off-tracking method: [5], [6]	Approximate linearization-based 'ghost-vehicle' approach: [10]	Input-output linearization approach: [9]	Cascaded-like control approach (proposed)
Type of considered vehicles	GNT	GNT (analyzed for $N \leq 2$)	nSNT	nSNT
Considered hitching offsets	$L_{hi} \geq 0$ for [6] L_{hi} in $\Re$ for [5] (with restrictions)	$L_{hi} \geq 0$ for N=2 or L_{hi} in $\Re$ for N=1	$L_{hi} > 0\ \forall i>0$ if $v<0$ or $L_{hi} \neq 0$ if $v>0$	$L_{hi} > 0\ \forall i>0$ or $L_{hi} < 0\ \forall i>0$
Admissible curvatures of reference paths	constant for [6], constant and varying for [5]	constant	constant	constant and **varying** (defined by F(x,y)=0)
Admissible motion strategy: F = forward B = backward	F for [6] F or B for [5]	F or B	F ($v>0$) if $L_{hi} \neq 0$ B ($v<0$) if $L_{hi} > 0$	F ($v>0$) if $L_{hi} < 0$ B ($v<0$) if $L_{hi} > 0$
Guidance point location: LT = last trailer TR = tractor	no single guidance point (non-classical approach)	on LT	on LT for $v<0$ on TR for $v>0$	**on LT**
Locality of control law definition	determined by linearization equations and path curvature	determined by linearization equations and path curvature	determined by linearization equations and path curvature	results only from points where $\|\nabla F(x,y)\|=0$ **(can be avoided)**
Stability	local, asymptotic	local, asymptotic	local, asymptotic	local, asymptotic
Determination of the shortest distance to the reference path	needed for all the vehicle segments	needed for the guidance segment	needed for the guidance segment	**not needed**
Controller scalability	high for [6] low for [5]	low	high	**high**
Controller tuning	simple	simple	simple	**very simple**

Figure 6: Qualitative comparison of the proposed cascaded-like control law with alternative PF control methods devised for N-trailers with off-axle hitching

[7]Therefore we do not discuss control laws proposed in [46, 48] and [42] which are devoted, respectively, to the differentially flat SNT kinematics, and to the multi-steered N-trailers (for the latter ones see also [52, 53]).

which are generically local). Only the proposed controller admits varying-curvature reference paths, simultaneously not requiring determination of the shortest distance to the path. Thanks to the cascade-like structure, scalability of the proposed controller is high. It means that complexity of equation (29) does not depend on a number of trailers present in a vehicle chain (in contrast to the controllers with low scalability, which have to be analytically resolved for the particular number of trailers). Control performance guaranteed for the guidance segment and tuning simplicity of the control law are fully inherited from the the outer-loop controller designed for unicycle kinematics in [39]. It makes the tuning process for the N-trailer as simple as for the unicycle preserving original control performance for the guidance segment (it explains description 'very simple' in the last row in Fig. 6). On the other hand, resultant control performance obtainable with linearization-based controllers substantially depends on poles location of the closed-loop dynamics; in this context, some practical difficulties with tuning of the controllers were reported in [9] and [10].

Practical restrictions of the proposed controller results from the fact that a reference path must be expressed by equation (7). Therefore, the non-analytical paths shall be first approximated by analytical formulas $f(x,y) = 0$ to be tractable by controller (29), cf. [39] for additional details in this context.

5. Experimental verification

5.1. Brief description of the experimental vehicle

Figure 7 presents the laboratory-scale articulated robotic vehicle used in experiments. The vehicle consists of a differentially driven tractor and up to three passive trailers of lengths $L_i = 0.229\,\text{m}$, $i = 1,2,3$. Joint angles are measured by 14-bit absolute encoders. Localization of the guidance segment is possible by an external vision system thanks to the active LED marker mounted on the last trailer. The vehicle has been equipped with TMS320F28335 digital signal processor allowing for computations of control law (29) entirely on a vehicle board with frequency $f_s = 100\,\text{Hz}$.

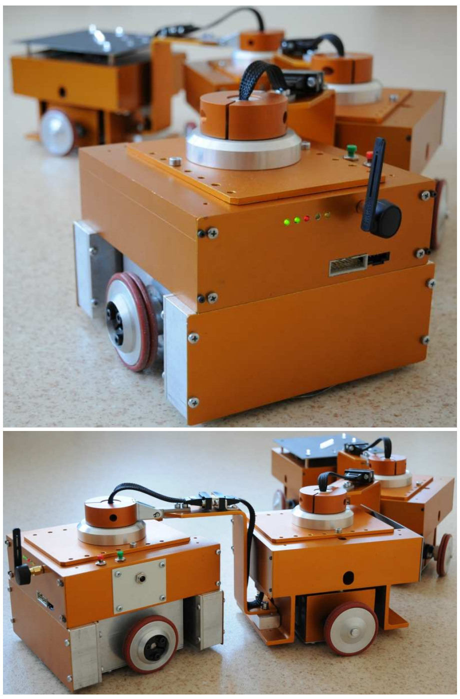

Figure 7: Three-trailer laboratory-scale robotic vehicle used in experiments

Angular velocities of tractor wheels are directly controlled by two PI-type velocity control loops implemented on the board. Hence, directly available control input to the tractor is a vector

$$\boldsymbol{\Omega}_d = \begin{bmatrix} \omega_{dR} \\ \omega_{dL} \end{bmatrix} = \boldsymbol{P}\,\boldsymbol{u}_0(\boldsymbol{\beta},\boldsymbol{\Phi}), \qquad \boldsymbol{P} = \begin{bmatrix} \frac{b}{2r} & \frac{1}{r} \\ -\frac{b}{2r} & \frac{1}{r} \end{bmatrix}, \tag{51}$$

where ω_{dR} and ω_{dL} denote desired angular velocities for the right and left tractor wheel, respectively, $\boldsymbol{u}_0(\boldsymbol{\beta},\boldsymbol{\Phi})$ has been defined by (29), while $b = 0.15\,\text{m}$ and $r \cong 0.029\,\text{m}$ are the tractor wheel base and the tractor wheel radius, respectively (cf. Fig. 1). To take into account actuator limits of the tractor, assume that $|\omega_{dR}(t)|$ and $|\omega_{dL}(t)|$ should not exceed in practice some prescribed bound $\omega_M > 0$ for all $t \geq 0$. To address this limit the following scaling procedure has been applied:

$$\boldsymbol{\Omega}_{ds}(t) \triangleq \frac{\boldsymbol{\Omega}_d(t)}{s(t)}, \qquad s(t) \triangleq \max\left\{1; \frac{|\omega_{dR}(t)|}{\omega_M}; \frac{|\omega_{dL}(t)|}{\omega_M}\right\} \tag{52}$$

where $s(t)$ is a scaling function such that $s(t) \geq 1$ for all $t \geq 0$. Procedure (52) guarantees that components of scaled angular velocity $\boldsymbol{\Omega}_{ds}(t)$ satisfy prescribed bound ω_M for all $t \geq 0$, simultaneously preserving desired motion curvature of a tractor. Scaled velocities of the tractor segment may be retrieved by inverse relation to (51), namely: $\boldsymbol{u}_{0s}(\boldsymbol{\beta},\boldsymbol{\Phi}) = [\omega_{0s}\ v_{0s}]^\top = \boldsymbol{P}^{-1}\boldsymbol{\Omega}_{ds} = \boldsymbol{u}_0(\boldsymbol{\beta},\boldsymbol{\Phi})/s(t)$, where the last equality results from combination of (52) and (51).

5.2. Results and comments

Two experiments, E1 and E2, have been conducted to illustrate control performance for varying-curvature S-P reference paths. The following common parameters have been selected for both tests: $L_{hi} = 0.048\,\text{m}$, $i = 1,2,3$, $v_d = -0.05\,\text{m/s}$, and $\omega_M = 10\,\text{rad/s}$. Experiment E1 was carried out using the elliptical reference path by taking $\sigma = +1$ and $f(x,y) \triangleq (x^2/A^2) + (y^2/B^2) - 1$ with $A = 0.7$ and $B = 0.5$. The outer-loop controller was implemented with design coefficients $k_1 = 2$ and $k_2 = 1$. Experiment E2 was performed for the sine-shaped reference path by taking $\sigma = -1$ and $f(x,y) \triangleq y - B\sin(Ax)$ with $A = 5.0$ and $B = 0.3$. In this case the outer-loop controller was implemented with design coefficients $k_1 = 20$ and $k_2 = 1$.

The results of experiments E1 and E2 are presented in Figs. 8 and 9, respectively. Apart from illustration of the robot motion in a task space, also the time plots of path-following errors F, e_θ, joint angles β_i, $i = 1,2,3$, scaled tractor velocities ω_{0s}, v_{0s}, and guidance-segment velocities ω_3, v_3 have been shown. Worth noting that initial positions of the guidance segment in the two experiments were selected in a much larger distance to the reference path than it would be admissible for the classical PF control approach proposed in [47] and commonly used for N-trailers, cf. [5, 6, 9, 10, 48]. Worth stressing smooth motion of the guidance segment, and stable evolution of the joint angles.

Robustness of the closed-loop system to parametric uncertainty of a vehicle kinematic model has been experimentally tested along the sine-shaped reference path, assuming both overestimated and underestimated values of trailer lengths and hitching offsets used in the inner-loop transformation (29). The results are presented in Fig. 10, where paths drawn by the guidance segment and time plots of PF error components $|f(\boldsymbol{q}_N(t))|$

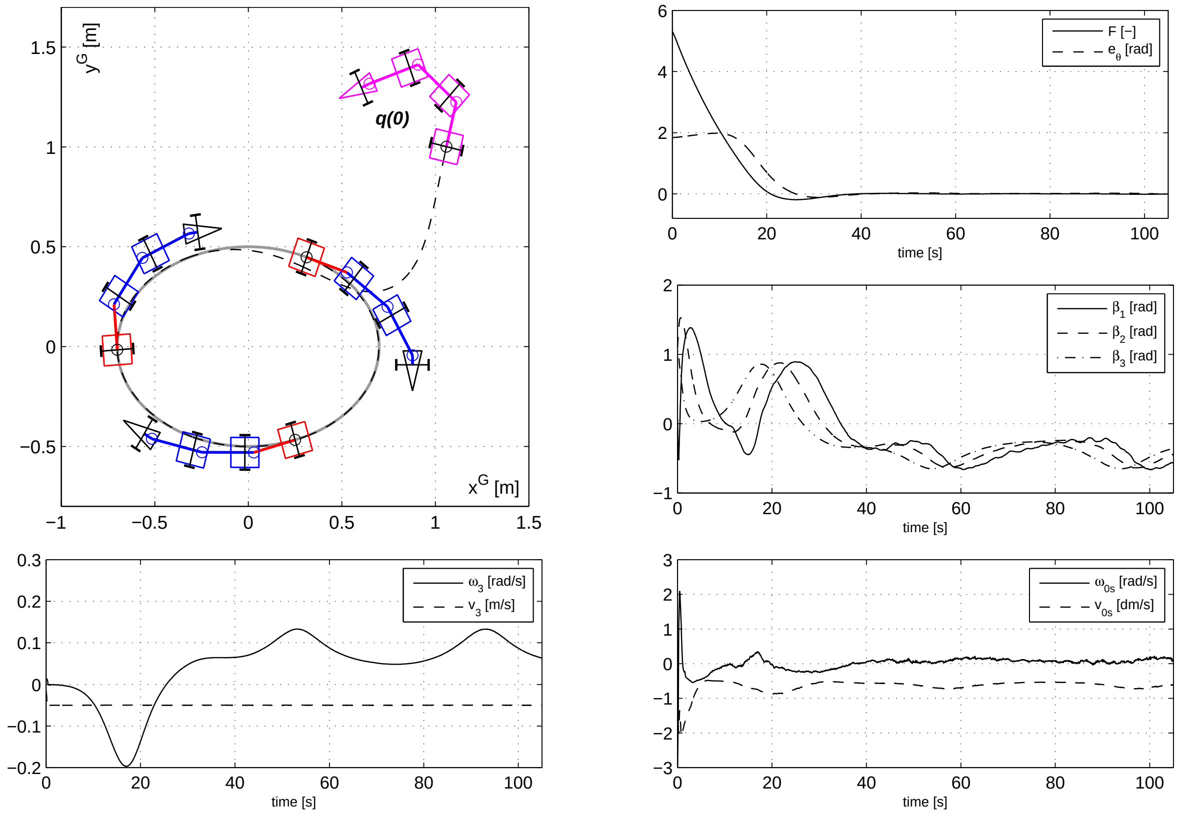

Figure 8: E1: Experimental results of following the elliptical reference path; the guidance segment has been highlighted in red, while initial vehicle configuration $\boldsymbol{q}(0)$ has been highlighted in magenta on X-Y plot

and $|e_\theta(t)|$ have been shown for the following cases: (a) using the *nominal* values of kinematic parameters and taking $\sigma = -4$, (b) using 10% overestimated trailers lengths and 10% underestimated hitching offsets, and taking $\sigma = -4$, (c) using 10% underestimated trailers lengths and 10% overestimated hitching offsets, and taking $\sigma = -4$, (d) using the same conditions as in case (b) but taking $\sigma = -8$. Comparing the plots in Fig. 10 one may claim relatively small sensitivity of the control system to parametric uncertainty of the vehicle model. Moreover, comparing the results for cases (b) and (d) one can see that increasing a value of $|\sigma|$ leads to improvement of the overall control performance despite the parametric uncertainty of the kinematic model.

6. Conclusions

The nonlinear cascaded-like state-feedback control law presented in the paper constitutes an alternative solution to the PF task for nSNT vehicles, where the reference paths can be expressed in the analytical form represented by (7). Thanks to utilization of the concept developed in [39], the proposed control law does not require determination of the shortest distance to a reference path, substantially simplifying practical application of the controller. By introducing of the so-called segment-platooning reference paths, it has been shown that the cascaded-like controller guarantees asymptotic following of both constant-curvature as well as some persistently exciting and sufficiently smooth varying-curvature reference paths. High scalability of the proposed controller allows its immediate application into N-trailers equipped with different numbers of sign-homogeneously off-axle hitched trailers. The novel control strategy admits either backward or forward motion of a vehicle (as a function of hitching offset signs), preserving location of the guidance point on the last trailer for both cases. Experimental results provided in the paper illustrated practical effectiveness of the new control law revealing its relatively small sensitivity to parametric uncertainty of a vehicle kinematic model.

Appendix A. Computation of function Atan2c (., .), [17]

Angle $\chi(t) = \text{Atan2c}\,(h_1(t), h_2(t)) \in \mathbb{R}$ for all $t \geq 0$ corresponds to a value of integral $\chi(t) = \chi(0) + \int_0^t [\dot{h}_1(\xi)h_2(\xi) - \dot{h}_2(\xi)h_1(\xi)]/[h_1^2(\xi) + h_2^2(\xi)]d\xi$ computed for appropriately selected initial condition $\chi(0)$. In the discrete-time domain $n \in \mathbb{N}$, a value of angle $\chi(n) = \text{Atan2c}\,(h_1(n), h_2(n))$ can be computed as follows:

1: $X(n) := \text{Atan2}\,(h_1(n), h_2(n)) \in (-\pi, \pi]$
2: $X(n-1) := \text{Atan2}\,(\sin\chi(n-1), \cos\chi(n-1)) \in (-\pi, \pi]$
3: $\Delta X(n) := X(n) - X(n-1)$
4: IF $\Delta X(n) > +\pi$ THEN $\Delta\chi(n) := \Delta X(n) - 2\pi$
ELSEIF $\Delta X(n) < -\pi$ THEN $\Delta\chi(n) := \Delta X(n) + 2\pi$
ELSE $\Delta\chi(n) := \Delta X(n)$
5: $\chi(n) := \chi(n-1) + \Delta\chi(n) \quad \Rightarrow \quad \chi(n) \in \mathbb{R}$

where $\chi(n-1)$ denotes a value from a previous time instant which should be stored in a memory.

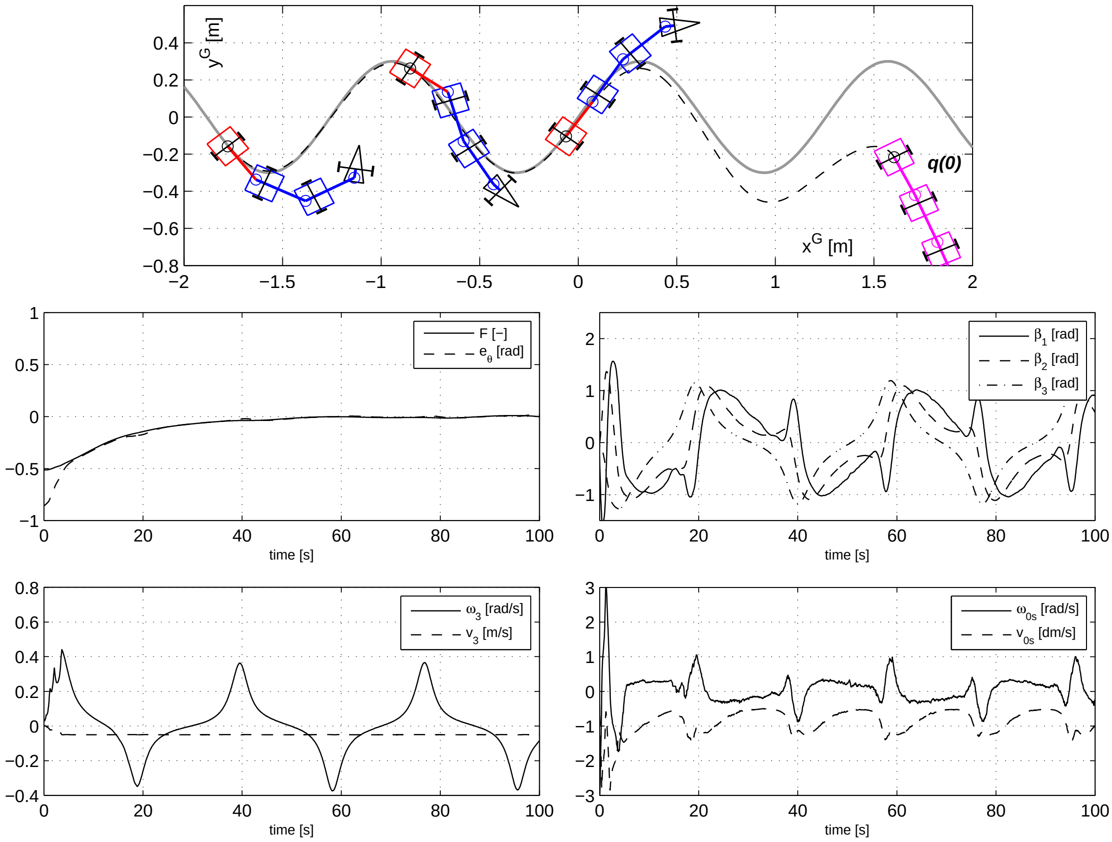

Figure 9: E2: Experimental results of following the sine-shaped reference path; the guidance segment has been highlighted in red, while initial vehicle configuration $\boldsymbol{q}(0)$ has been highlighted in magenta on X-Y plot

Appendix B. Some explanations for S-P paths

Let us show equivalence between conditions (13) and (15). Since $\tan\delta_{di}(t) = L_i\kappa_{di}(t)$ and curvature $\kappa_{di}(t) = \omega_{di}(t)/v_{di}(t)$, one may rewrite (15) as $L_i\omega_{di}(t)v_{di}(t)\tan\beta_{di}(t) + v_{di}^2(t) > 0$. Upon (11) we have $|\beta_{di}(t)| < \pi/2$, thus the latter inequality can be multiplied by $\cos\beta_{di}(t)$ and reformulated as $v_{di}(t)(L_i\omega_{di}(t)\sin\beta_{di}(t) + v_{di}(t)\cos\beta_{di}(t)) > 0$. Since $(L_i\omega_{di}(t)\sin\beta_{di}(t) + v_{di}(t)\cos\beta_{di}(t)) = v_{di-1}(t)$ (according to (14) and (4)), hence condition (15) is equivalent to relation (13).

We are going to derive a relation between reference velocities v_{di-1} and v_{di} for the case of circular reference paths. It is known that for the steady-state circular motion of the N-trailer the following two equalities are valid (see [35]): $\omega_{di} = (v_{di-1}\mathrm{s}\beta_{di})/(L_i + L_{hi}\mathrm{c}\beta_{di})$ and $v_{di-1} = (v_{di} - \omega_{di}L_{hi}\mathrm{s}\beta_{di})/\mathrm{c}\beta_{di}$. Combining the two equations yields $\omega_{di} = (v_{di}\mathrm{s}\beta_{di})/(L_{hi} + L_i\mathrm{c}\beta_{di})$. By substituting the latter into the second row of propagation formula $\boldsymbol{u}_{di-1} = \boldsymbol{J}_i^{-1}(\beta_{di})\boldsymbol{u}_{di}$ (cf. (4)) gives relation $v_{di-1} = v_{di}\cdot(L_i + L_{hi}\mathrm{c}\beta_{di})/(L_i\mathrm{c}\beta_{di} + L_{hi})$.

Appendix C. Stability lemma for LTV systems

Following [44] and [56] let us recall the useful stability lemma for LTV systems, which has been slightly reformulated here for the case of matrices possessing only real eigenvalues.

Lemma 2. *Consider the LTV system $\dot{\boldsymbol{x}} = \boldsymbol{A}(t)\boldsymbol{x}$ where $\boldsymbol{A}(t) : \mathbb{R}_+ \mapsto \mathbb{R}^{n\times n}$ has solely real eigenvalues $\lambda_i(\boldsymbol{A}(t))$, $i = 1,\dots,n$. Assume that there exists $\bar{A} > 0$ such that $\|\boldsymbol{A}(t)\| \le \bar{A}$ for all $t \ge 0$, and there exists a constant $\alpha > 0$ such that $\lambda_i(\boldsymbol{A}(t)) \le -\alpha$ for all $t \ge 0$ and all $i = 1,\dots,n$. The sufficient condition for exponential stability of LTV system at $\boldsymbol{x} = \boldsymbol{0}$ is the existence of sufficiently small constant $\delta_A > 0$ such that*

$$\forall\, t \ge 0 \quad \left\|\dot{\boldsymbol{A}}(t)\right\| \le \delta_A. \tag{C.1}$$

The above lemma provides the sufficient condition (not the necessary one), thus (C.1) may be conservative (cf. [56]).

Acknowledgement 1. *The author is indebted to Dr. Eng. Marcin Kiełczewski from Chair of Control and Systems Engineering (PUT) for a help in collecting the experimental data. He also thanks for critical and motivating comments provided by the anonymous reviewers.*

References

[1] A. P. Aguiar and J. P. Hespanha. Trajectory-tracking and path-following of underactuated autonomous vehicles with parametric modeling uncertainty. *IEEE Trans. Automatic Control*, 52(8):1362–1379, 2007.

[2] A. P. Aguiar, J. P. Hespanha, and P. V. Kokotović. Performance limitations in reference-tracking and path-following for nonlinear systems. *Automatica*, 44:598–610, 2008.

[3] M. Aicardi, G. Casalino, A. Bicchi, and A. Balestrino. Closed loop steering of unicycle-like vehicles via Lyapunov techniques. *IEEE Robotics & Automation Magazine*, 2:27–35, 1995.

[4] C. Altafini. Some properties of the general n-trailer. *Int. Journal of Control*, 74(4):409–424, 2001.

[5] C. Altafini. Following a path of varying curvature as an output regulation problem. *IEEE Trans. on Automatic Control*, 47(9):1551–1556, 2002.

[6] C. Altafini. Path following with reduced off-tracking for multibody wheeled vehicles. *IEEE Trans. on Control Systems Technology*, 11(4):598–605, 2003.

[7] C. Altafini, A. Speranzon, and B. Wahlberg. A feedback control scheme for reversing a truck and trailer vehicle. *IEEE Transactions on Robotics and Automation*, 17(6):915–922, 2001.

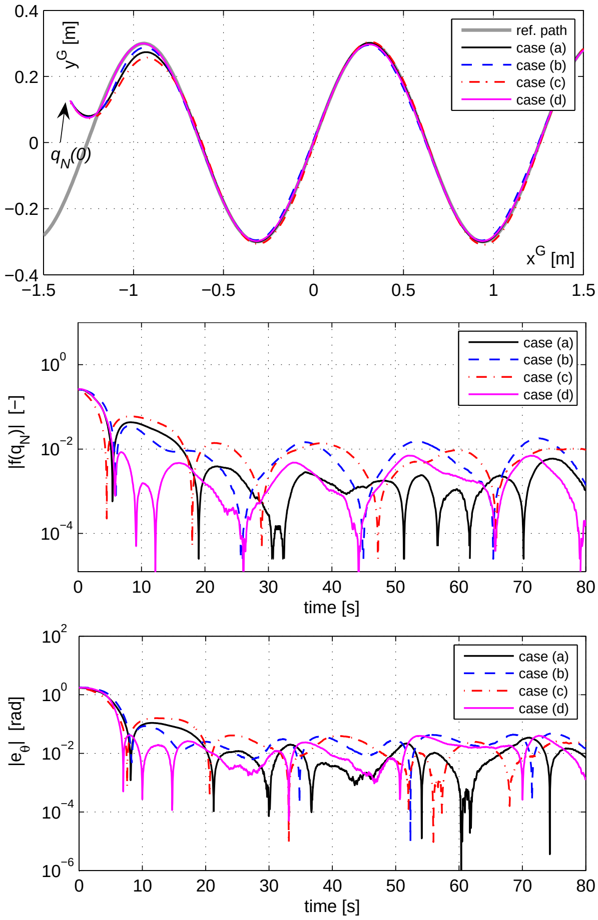

Figure 10: Robustness tests: paths drawn by the guidance segment and logarithmic plots of PF error components obtained for sine-shaped reference path under nominal conditions – case (a), and in the presence of 10% parametric uncertainty of a vehicle kinematic model – cases (b) to (d), see Section 5.2

[8] A. Astolfi, P. Bolzern, and A. Locatelli. Path-tracking of a tractor-trailer vehicle along rectilinear and circular paths: a Lyapunov-based approach. *IEEE Trans. on Robotics and Automation*, 20(1):154–160, 2004.

[9] P. Bolzern, R. M. DeSantis, and A. Locatelli. An input-output linearization approach to the control of an n-body articulated vehicle. *Journal of Dynamic Systems, Measurement, and Control*, 123:309–316, 2001.

[10] P. Bolzern, R. M. DeSantis, A. Locatelli, and D. Masciocchi. Path-tracking for articulated vehicles with off-axle hitching. *IEEE Trans. on Control Systems Technology*, 6(4):515–523, 1998.

[11] L. Bushnell, B. Mirtich, A. Sahai, and M. Secor. Off-tracking bounds for a car pulling trailers with kingpin hitching. In *Proceedings of the 33rd Conference on Decision and Control*, pages 2944–2949, Lake Buena Vista, USA, 1994.

[12] C. Canudas-de-Wit and A. D. NDoudi-Likoho. Nonlinear control for a convoy-like vehicle. *Automatica*, 36:457–462, 2000.

[13] C. Cariou, R. Lenain, B. Thuilot, and P. Martinet. Path following of a vehicle-trailer system in presence of sliding: Application to automatic guidance of a towed agricultural implement. In *The 2010 IEEE/RSJ Int. Conf. Intel. Robots and Systems*, pages 4976–4981, Taiwan, 2010.

[14] W. Chung, M. Park, K. Yoo, J. I. Roh, and J. Choi. Backward-motion control of a mobile robot with n passive off-hooked trailers. *J. Mechanical Science and Technology*, 25(11):2895–2905, 2011.

[15] L. Consolini, M. Maggiore, C. Nielsen, and M. Tosques. Path following for the PVTOL aircraft. *Automatica*, 46:1284–1296, 2010.

[16] R. M. DeSantis, J. M. Bourgeot, J. N. Todeschi, and R. Hurteau. Path-tracking for tractor-trailers with hitching of both the on-axle and the off-axle kind. In *Proc. of the 2002 IEEE Int. Symp. on Intelligent Control*, pages 206–211, Vancouver, Canada, 2002.

[17] M. Michałek and M. Kiełczewski. Cascaded VFO set-point control for N-trailers with on-axle hitching. *IEEE Trans. Control Systems Technology*, 2013. DOI: 10.1109/TCST.2013.2290770.

[18] A. Ferrara and L. Magnani. Hybrid variable structure path tracking control of articulated vehicles. In *Proc. of the 2004 American Control Conference*, pages 2777–2782, Boston, USA, 2004.

[19] C.-J. Hoel and P. Falcone. Low speed maneuvering assistance for long vehicle combinations. In *2013 IEEE Intell. Vehicles Symp.*, pages 598–604, Gold Coast, Australia, 2013.

[20] F. Jean. The car with N trailers: characterisation of the singular configurations. *Control, Opt. Calc. Variations*, 1:241–266, 1996.

[21] B. A. Jujnovich and D. Cebon. Path-following steering control for articulated vehicles. *Journal of Dynamic Systems, Measurement, and Control*, 135(3), 2013. DOI: 10.1115/1.4023396.

[22] Y. Kim and M. A. Minor. Path manifold-based kinematic control of wheeled mobile robots considering physical constraints. *Int. J. Robotics Research*, 26(9):955–975, 2007.

[23] F. Lamiraux, S. Sekhavat, and J. Laumond. Motion planning and control for Hilare pulling a trailer. *IEEE Trans. on Robotics and Automation*, 15(4):640–652, 1999.

[24] L. Lapierre, D. Soetanto, and A. Pascoal. Nonsingular path following control of a unicycle in the presence of parametric modelling uncertainties. *Int. J. Robust Nonlinear Control*, 16:485–503, 2006.

[25] J. P. Laumond. Controllability of a multibody mobile robot. *IEEE Transactions on Robotics and Automation*, 9(6):755–763, 1993.

[26] J. Lee, W. Chung, M. Kim, C. Lee, and J. Song. A passive multiple trailer system for indoor service robots. In *Proceedings of the 2001 IEEE/RSJ International Conference on Intelligent Robots amd Systems*, Maui, Hawaii, 2001.

[27] Z. Leng and M. Minor. A simple tractor-trailer backing control law for path following. In *The 2010 IEEE/RSJ Int. Conf. Intell. Robots and Systems*, pages 5538–5542, Taipei, Taiwan, 2010.

[28] P. Liljebäck, I. U. Haugstuen, and K. Y. Pettersen. Path following control of planar snake robots using a cascaded approach. *IEEE Trans. on Control Systems Technology*, 20(1):111–126, 2012.

[29] D. A. Lizarraga, P. Morin, and C. Samson. Chained form approximation of a driftless system. Application to the exponential stabilization of the general n-trailer system. *International Journal of Control*, 74(16):1612–1629, 2001.

[30] J. L. Martinez, M. Paz, and A. Garcia-Cerezo. Path tracking for mobile robots with a trailer. In *15th Triennial IFAC World Congress*, pages 865–865, Barcelona, Spain, 2002.

[31] R. T. M'Closkey and R. M. Murray. Experiments in exponential stabilization of a mobile robot towing a trailer. In *Proc. of the American Control Conference*, pages 988–993, Baltimore, USA, 1994.

[32] M. Michałek. Application of the VFO method to set-point control for the N-trailer vehicle with off-axle hitching. *Int. Journal of Control*, 85(5):502–521, 2012.

[33] M. Michałek. Cascaded approach to the path-following problem for N-trailer robots. In *Proc. 9th Int. Workshop on Robot Motion and Control*, pages 161–166, Wasowo Palace, Poland, 2013.

[34] M. Michałek. Lining-up control strategies for N-trailer vehicles. *J. Intell. Robot. Syst.*, 2013. DOI: 10.1007/s10846-013-9846-2.

[35] M. Michałek. Non-minimum-phase property of N-trailer kinematics resulting from off-axle interconnections. *Int. Journal of Control*, 86(4):740–758, 2013.

[36] J. Morales, J. L. Martinez, A. Mandow, and A. J. Gracia-Cerezo. Steering the last trailer as a virtual tractor for reversing vehicles with passive on- and off-axle hitches. *IEEE Trans. Industrial Electronics*, 60(12):5729–5736, 2013.

[37] J. Morales, J. L. Martinez, A. Mandow, and I. J. Medina. Virtual steering limitations for reversing an articulated vehicle with off-axle passive trailers. In *35th Annual Conf. of IEEE Ind. Electronics*, pages 2385–2390, Porto, Portugal, 2009.

[38] J. Morales, J. L. Martínez, M. A. Martínez, and A. Mandow. Pure-pursuit reactive path tracking for nonholonomic mobile robots with a 2D laser scanner. *EURASIP J. Advances in Signal Processing*, pages 1–10, 2009. DOI:10.1155/2009/935237.

[39] A. Morro, A. Sgorbissa, and R. Zaccaria. Path following for unicycle robots with arbitrary path curvature. *IEEE Trans. on Robotics*, 27(5):1016–1023, 2011.

[40] B. Murugendran, A. A. Transeth, and S. A. Fjerdingen. Modeling and path-following for a snake robot with active wheels. In *The 2009 IEEE/RSJ Int. Conf. Intell. Robots and Systems*, pages 3643–3650, St. Louis, USA, 2009.

[41] M. Nakamura and S. Yuta. Trajectory control of trailer type mobile robot. In *Proc. of the IEEE/RSJ Int. Conf. on Intel. Robots and Systems*, pages 2257–2263, Yokohama, Japan, 1993.

[42] R. Orosco-Guerrero, E. Aranda-Bricaire, and M. Velasco-Villa. Global path-tracking for a multi-steered general N-trailer. In *Proc. 15th IFAC Triennial World Congress*, pages 239–239, Barcelona, Spain, 2002.

[43] P. Petrov. Nonlinear backward tracking control of an articulated mobile robot with off-axle hitching. In *Proc. of the 9th WSEAS International*

Conf. on Signal Processing, Robotics and Automation, pages 269–273, 2010.

[44] H. H. Rosenbrock. The stability of linear time-dependent control systems. *J. Electronics and Control*, 15(1):73–80, 1963.

[45] P. Rouchon, M. Fliess, J. Levine, and P. Martin. Flatness, motion planning and trailer systems. In *Proceedings of the 32nd Conference on Decision and Control*, pages 2700–2705, San Antonio, USA, 1993.

[46] M. Sampei, T. Tamura, T. Kobayashi, and N. Shibui. Arbitrary path tracking control of articulated vehicles using nonlinear control theory. *IEEE Trans. on Control Systems Technology*, 3(1):125–131, 1995.

[47] C. Samson. Path following and time-varying feedback stabilization of a wheeled mobile robot. In *Proc. Int. Conf. ICARCV'92*, pages 13.1.1–13.1.5, Singapore, 1992.

[48] C. Samson. Control of chained systems. Application to path following and time-varying point-stabilization of mobile robots. *IEEE Trans. on Automatic Control*, 40(1):64–77, 1995.

[49] A. Sgorbissa and R. Zaccaria. Integrated obstacle avoidance and path following through a feedback control law. *J. Intell. Robot. Syst.*, 72:409–428, 2013.

[50] S. Skogestad and I. Postlethwaite. *Multivariable feedback control. Analysis and design. 2nd Ed.* Wiley, West Sussex, 2005.

[51] B. Thuilot, C. Cariou, P. Martinet, and M. Berducat. Automatic guidance of a farm tractor relying on a single CP-DGPS. *Auton. Robots*, 13:53–71, 2002.

[52] D. Tilbury, O. J. Sordalen, L. Bushnell, and S. S. Sastry. A multisteering trailer system: Conversion into chained form using dynamic feedback. *IEEE Trans. Robotics and Automation*, 11(6):807–818, 1995.

[53] J. Yuan, Y. Huang, Y. Kang, and Z. Liu. A strategy of path following control for multi-steering tractor-trailer mobile robot. In *Proc. 2004 IEEE Int. Conf. Robotics and Biomimetics*, pages 163–168, Shenyang, China, 2004.

[54] J. Yuan, Y. Huang, and F. Sun. Design for physical structure of tractor-trailer mobile robot. In *Proc. 2004 IEEE Int. Conf. Robotics and Biomimetics*, pages 511–516, Shenyang, China, 2004.

[55] Z. Zheng, W. Huo, and Z. Wu. Autonomous airship path following control: Theory and experiments. *Control Engineering Practice*, 21:769–788, 2013.

[56] J. J. Zhu. A note on extension of the eigenvalue concept. *IEEE Control Systems*, 13(6):68–70, 1993.